DESIGN AND ANALYSES OF TALL TAPERED REINFORCED CONCRETE CHIMNEYS SUBJECTED TO EARTHQUAKE

By Nelson M. Isada *, Ph.D.

0. INTRODUCTION

The object of this paper is to summarize rational and workable rules to follow in the design and dynamic analyses of tall tapered reinforced concrete chimneys on rigid foundations as determined by earthquake stresses. The structural properties of three chimneys designed in the United States are used.

The study is divided into three major phases. The first involves the accumulation of accelerogram records and experimental results on the coefficient of damping. The second phase is the series of dynamic analytical studies which includes the derivation of the dynamic equations, fundamental mode structural properties, second and higher modes structural properties, solution of the generalized co-ordinate differential equations, determination of the maximum shears and bending moments, and determination of the magnification factors which are compared to the ACI (49-26) Code. The third phase is the determination of the suggested design formulas.

I. ACCELEROGRAMS AND DAMPING COEFFICIENTS

From the work of Alford, J. L., et al, (1), on "spectrum analyses", it is decided to use three accelerogram records. The first accelerogram chosen is the record taken at El Centro, California, on May 18, 1940, with N-S component. This accelerogram takes care of the localities where the maximum acceleration recorded is 0.09g or more. The second accelerogram chosen is the record taken at Vernon, California, on October 2, 1933, with N08E component. This covers localities whose recorded accelerograms show maximum accelerations of from 0.05g to 0.09g. The third accelerogram chosen is the record taken at the Los Angeles Subway Terminal on October 2, 1953, with N39E component. This accelerogram covers localities whose accelerogram records show maximum accelerations of less than 0.05g.

Hisada, T. (2), Merritt, G. (3), White, M. P. (4), and others have studied and performed experiments to determine the values of the coefficient of damping. From their studies it has been concluded that 5% and 7½% of critical damping for each mode should be used in this study.

II. DYNAMIC EQUATIONS

The lateral vibration of a beam is analyzed (5) with the following assumptions:

(1) The cross section of the beam is small compared to its length so

---

* Senior Structural Engineer of Smith, Hinchman & Grylls, Inc., Detroit, Michigan. Former Research Assistant & Teaching Fellow, University of Michigan, Ann Arbor, Mich.

that the effect of shear and rotary inertia on the configuration of the beam may be neglected.

(2) The beam is elastic.

The beam equations below are found in books on mechanics of vibration (5)*:

$$EI\frac{\partial^2 y}{\partial x^2} = -M, \qquad \ldots\ldots\ldots\ldots (2.1)$$

$$\frac{d}{dx}\left(EI\frac{\partial^2 y}{\partial x^2}\right) = -\frac{dM}{dx} = -V, \qquad \ldots\ldots\ldots\ldots (2.2)$$

$$\frac{d^2}{dx^2}\left(EI\frac{\partial^2 y}{\partial x^2}\right) = -\frac{dV}{dx} = W, \qquad \ldots\ldots\ldots\ldots (2.3)$$

where

E = Young's modulus of elasticity,
I = moment of inertia,
x = distance from base to a general point P on neutral axis of bending,
y = lateral displacement of neutral axis of bending,
M = bending moment,
V = shear,
W = load per unit length.

If the beam is vibrating, the load per unit length W of eq. (2.3) is the inertia force per unit length. By Newton's principle the load per unit length is

$$W = -\frac{w}{g}\frac{\partial^2 y}{\partial t^2} = -m\frac{\partial^2 y}{\partial t^2}, \qquad \ldots\ldots\ldots\ldots (2.4)$$

where

w = weight per unit length,
t = time variable,
m = mass per unit length along the beam.

Substitution of eq. (2.4) into eq. (2.3) yields

$$\frac{d^2}{dx^2}\left(EI\frac{\partial^2 y}{\partial x^2}\right) = -m\frac{\partial^2 y}{\partial t^2}, \qquad \ldots\ldots\ldots\ldots (2.5)$$

which is the general equation for the free lateral vibration of beams without damping.

Now consider the case when there is ground motion, say during an earthquake. Let

$y_b(t)$ = motion of the base,
$Y_x(t)$ = horizontal absolute motion of the xth point along the neutral axis of bending of the beam,
$y_x(t)$ = motion of the xth point relative to the base.

Thus,

$$Y_x(t) = y_b(t) + y_x(t). \qquad \ldots\ldots\ldots\ldots (2.6)$$

Since the inertia force in eq. (2.5) is based on absolute acceleration, eq. (2.4) becomes

$$\frac{d^2}{dx^2}\left(EI\frac{\partial^2 y}{\partial x^2}\right) = -m\left(\frac{\partial^2 y}{\partial t^2} + \frac{\partial^2 y_b}{\partial t^2}\right). \qquad \ldots\ldots\ldots\ldots (2.7)$$

Lagrange's equation (5) is used to reduce eq. (2.7) into a different form. This equation for free vibration is

---

* This and subsequent numbers in parenthesis refer to the bibliography.

$$\frac{d}{dt}\left(\frac{\partial T}{\partial \dot{q}_j}\right) - \frac{\partial T}{\partial q_j} + \frac{\partial U}{\partial q_j} = 0, \qquad \cdots\cdots (2.8)$$

where

T = total kinetic energy of the whole system,

q_j = jth generalized co-ordinate,

U = total potential energy of the whole system, which is a function of the configuration of the system only,

$$\dot{q}_j = \frac{dq_j}{dt}.$$

Now, let

$$y_j = Z_j(x) q_j(t) \qquad \cdots\cdots (2.9)$$

be a solution of eq. (2.7). Superposition of all possible solutions gives the general solution

$$y = \sum_{j=1}^{\infty} Z_j q_j. \qquad \cdots\cdots (2.10)$$

Therefore, the expression for the potential energy of a bent beam is

$$U = \frac{1}{2}\int_0^h EI\left(\frac{\partial^2 y}{\partial x^2}\right)^2 dx, \qquad \cdots\cdots (2.11)$$

or,

$$U = \frac{1}{2}\int_0^h EI\left(\sum_{j=1}^{\infty} \ddot{Z}_j q_j\right)^2 dx, \qquad \cdots\cdots (2.11a)$$

or,

$$U = \frac{1}{2}\int_0^h EI\left(\ddot{Z}_1 q_1 + \ddot{Z}_2 q_2 + \cdots + \ddot{Z}_\infty q_\infty\right)^2 dx \qquad \cdots\cdots (2.11b)$$

Let Z_j and $\ddot{Z}_j$ be orthogonal functions with respect to the weight function m, i.e.,

$$\int_0^h m Z_r Z_s \, dx = 0, \quad \text{when } r \neq s, \qquad \cdots\cdots (2.12)$$

and

$$\int_0^h m \ddot{Z}_r \ddot{Z}_s \, dx = 0, \quad \text{when } r \neq s. \qquad \cdots\cdots (2.12a)$$

Since EI can be expressed in terms of m and the terms containing the products $\ddot{Z}_r\ddot{Z}_s$ when r is not equal to s vanish according to eq. (2.12a), eq. (2.11b) reduces to

$$U = \frac{1}{2}\int_0^h EI \sum_{j=1}^{\infty} \ddot{Z}_j^2 q_j^2 \, dx. \qquad \cdots\cdots (2.13)$$

Since $\ddot{Z}_j$ are functions of x alone and q_j are functions of t alone, eq. (2.13) becomes

$$U = \frac{1}{2}\sum_{j=1}^{\infty} q_j^2 \int_0^h EI(\ddot{Z}_j)^2 dx, \qquad \cdots\cdots (2.14)$$

and

$$\frac{\partial U}{\partial q_j} = q_j \int_0^h EI \ddot{Z}_j^2 dx. \qquad \cdots\cdots (2.15)$$

The expression for the kinetic energy during an earthquake is

$$T = \frac{1}{2}\int_0^h m\left(\frac{\partial Y}{\partial t}\right)^2 dx, \qquad \cdots\cdots (2.16)$$

or

$$T = \frac{1}{2}\int_0^h m\left[\dot{y}_b + \sum_{j=1}^{\infty} Z_j \dot{q}_j\right]. \qquad \cdots\cdots (2.16a)$$

Because the terms containing Z_rZ_s vanish when $r \neq s$ according to eq. (2.43), eq. (2.16a) becomes

$$T = \frac{1}{2}\dot{y}_b^2 \int_0^h m dx + \dot{y}_b \sum_{j=1}^{\infty} \dot{q}_j \int_0^h m Z_j dx + \frac{1}{2}\sum_{j=1}^{\infty} \dot{q}_j^2 \int_0^h m Z_j^2 dx, \qquad \cdots (2.16b)$$

and

$$\frac{\partial T}{\partial \dot{q}_j} = \dot{y}_b \int_0^h m Z_j dx + \dot{q}_j \int_0^h m Z_j^2 dx. \qquad \cdots\cdots (2.17)$$

Thus,

$$\frac{d}{dt}\left(\frac{\partial T}{\partial \dot{q}_j}\right) = \ddot{y}_b \int_0^h m Z_j \, dx + \ddot{q}_j \int_0^h m Z_j^2 \, dx . \qquad \ldots\ldots\ldots (2.18)$$

and

$$\frac{\partial T}{\partial q_j} = 0 . \qquad \ldots\ldots\ldots (2.19)$$

Hence, Lagrange's equation for the jth mode of a tall tapered chimney during an earthquake without damping is

$$\ddot{y}_b \int_0^h m Z_j \, dx + \ddot{q}_j \int_0^h m Z_j^2 \, dx - q_j \int_0^h E I \ddot{Z}_j^2 \, dx = 0 , \qquad \ldots\ldots (2.20)$$

or,

$$\ddot{q}_j + \omega_j^2 q_j = - \Gamma_j \ddot{y}_b , \qquad \ldots\ldots (2.21)$$

where

$$\omega_j^2 = - \frac{\int_0^h E I \ddot{Z}_j^2 \, dx}{\int_0^h m Z_j^2 \, dx} , \qquad \ldots\ldots (2.22)$$

$$\Gamma_j = \frac{\int_0^h m Z_j \, dx}{\int_0^h m Z_j^2 \, dx} . \qquad \ldots\ldots (2.23)$$

The practice in taking damping into account is to introduce damping assumed effectively to be viscous, for each mode. This is done by introducing a fraction of critical damping for the particular mode. The term is $2\beta_j \omega_j \dot{q}_j$ where β_j is the fraction of critical damping.

With the viscous damping term, eq. (2.21) becomes

$$\ddot{q}_j + 2\beta_j \omega_j \dot{q}_j + \omega_j^2 q_j = - \Gamma_j \ddot{y}_b , \qquad \ldots\ldots (2.24)$$

or

$$\ddot{\phi}_j + 2\beta_j \omega_j \dot{\phi}_j + \omega_j^2 \phi_j = - \ddot{y}_b , \qquad \ldots\ldots (2.25)$$

where

$$\phi_j = q_j / \Gamma_j . \qquad \ldots\ldots (2.26)$$

Therefore, the general solution of eq. (2.7) may be obtained from the solutions of eq. (2.25) which is

$$y = \sum_{j=1}^{\infty} Z_j \Gamma_j \phi_j . \qquad \ldots\ldots (2.27)$$

The procedures in getting the values of Z_j, Γ_j and ϕ_j are discussed later. In getting the values of Z_j, the corresponding Shear V_j and Bending Moment M_j factors for a unit Z_j at the top of the stack are also derived. Hence, if the shear V_j and moment M_j factors for each mode are known, then the total shear V and moment M may be obtained by adding the effect of each mode, i.e.,

$$V = \sum_{j=1}^{\infty} V_j y_{ej} = \sum_{j=1}^{\infty} V_j \Gamma_j \phi_j , \qquad \ldots\ldots (2.28)$$

and

$$M = \sum_{j=1}^{\infty} M_j \Gamma_j \phi_j . \qquad \ldots\ldots (2.29)$$

III. DYNAMIC STRUCTURAL PROPERTIES: FUNDAMENTAL MODE

Any elastic curve $y(x)$ which may be induced in the stack can be split up into a series of "orthogonal" curves (6). To find these elastic curves (Z_j) which are oftentimes called mode shapes, Stodola's method is essentially used. A modification based upon Newmark's assumption of regional parabolic

shape of elastic and inertia load curves is used in the integration processes to find the derived elastic curve.

This modified Stodola's method (7) is briefly divided into different steps below:

1. Divide the stack into equal segments and then record the mass intensities, concentrated masses, moment of inertias, and length of each segment as shown in Fig. 3.1. Note that in Fig. 3.1 there is a column at the extreme right marked "Multiplier". This multiplier is used simply to avoid large figures;

2. Assume a reasonable deflection curve $Z_i(x)$. This assumed deflection curve must be based upon previous studies made in the field. Since there is hardly any data available regarding the natural mode shapes of tapered chimneys, it is hoped that this study will be of some use, at least as a guide for this purpose as well as in analysis and design;

3. Compute the inertia load. Since damping has been found to have negligible effect on the inertia load (7), the inertia load $m\omega_i^2 Z_i$ is obtained by multiplying the assumed deflections by the product of the mass and the square of the unknown frequency. Equivalent concentrated inertia loads are computed and the results are added to the additional concentrated inertia loads due to the concentrated masses. Newmark's method of integration (8) is used to get the equivalent concentrated inertia loads from the inertia load per unit length;

4. Having found the inertia loads, the deflected curve can then be constructed by means of the conjugate beam, graphical statics, or Newmark's method. Actually, the three methods are based on the same basic steps of integration of the inertia load $-m\omega_i^2 Z_i$ twice and division of the results by EI and then integrated two times more. The inertia load W_j is integrated once to arrive at the shear V_j and integrated once more to arrive at the bending moment M_j. Integration of the M_j/EI-diagram twice gives the deflected curve Z_j. The Newmark method (9) affords an orderly arrangement and a very rapid means of making these integration procedures, which gives as its final result the deflected curve Z_j. The difference from the conjugate beam method is the fact that the inertia load is assumed to be regionally parabolic instead of a straight line and that the figures used in the computations are tabulated.

Newmark's three reaction formulas used to compute the concentrated inertia loads due to the distributed inertia loads are:

$$R_{ab} = \frac{\lambda}{12}(3.5a + 3b - 0.5c), \qquad \ldots\ldots\ldots (3.1)$$

$$R_b = \frac{\lambda}{12}(a + 10b + c), \qquad \ldots\ldots\ldots (3.2)$$

$$R_{cb} = \frac{\lambda}{12}(3.5c + 3b - 0.5c). \qquad \ldots\ldots\ldots (3.3)$$

where a, b, and c are ordinates of the parabolic curve. The concentrated inertia loads, which are computed from the distributed inertia loads, are added to the concentrated inertia loads caused by the concentrated masses like floors, corbels, and water tank. Since the shear at the top of the stack (the free end) is zero, the total concentrated loads are summed from top to bottom to get the average shears at the mid-points of the various adjacent stations along the stack. After the shear is found, one can easily

compute the bending moments at any station along the stack by recalling that the area under the shear diagram is the bending moment. Since the segments are of equal length which is denoted by λ the bending moment contributed by each segment is the average shear multiplied by λ which is the area of the shear diagram for that segment. Therefore, to get the bending moment, the average shears are summed from top to bottom since again the bending moment at the top of the stack is also zero (free end). The factor λ is also taken out and is incorporated with the previous multiplier. Then divide the bending moment diagram by EI and compute the concentrated M_1/EI values by using the same procedure that is used in computing the concentrated inertia loads. These concentrated $\frac{M}{EI}$-values are summed from bottom (zero slope) to the top of the stack. Similarly, the area under this slope-diagram is the deflection, the order of summation being from bottom (fixed end) to the top of the stack.

5. If the derived deflection curve $Z_1(x)$ coincides with the originally assumed deflection curve $Z(x)$ then $Z_1(x)$ is exactly the normal elastic curve. If, however, the derived $Z_1(x)$ does not coincide with the assumed $Z(x)$ then steps (2), (3), and (4) are repeated, only this time the derived $Z_1(x)$ from the previous trial is used as the assumed deflection curve. The procedure is a very rapidly converging process for the fundamental mode (6).

6. The natural frequency is obtained from the fundamental mode shape arrived at by using steps (1) to (5). For example, in Fig. 3.1, at the top of the stack the way to obtain the natural frequency is by using the relationship

$$1.0\, Z_{e1} = c\,\frac{\lambda^4 \omega_1^2 Z_{e1}}{144 E I_e g}\,, \qquad \ldots\ldots\ldots (3.4)$$

where

λ = length of segment,
c = figure arrived at the top of the stack by steps (1) to (5),
g = acceleration due to gravity,
E = modulus of elasticity,
I_e = moment of inertia at the top of the stack.

In this Stodola-Newmark's method, the effect of shear along the height of the stack and the rocking or rotation of the base are neglected, although they may be considered (7, 18, 19).

As a numerical example, consider the computations shown in Fig. 3.1. Line 1 is the station designation. Line 2 is the distributed weight per unit length. Line 3 is the EI value. Line 4 is the assumed deflection curve. Multiply the figures in line 2 by the corresponding figures in line 5 to get line 6, and at the same time multiply the multiplier by ω_1^2/g. Line 7 is obtained from line 6 by Newmark's method of integration discussed previously. For example for station e, line 7 becomes

$$(3.5 \times 7.500 + 3.0 \times 7.591 - 0.5 \times 6.954)\left[\lambda \omega_1^2 Z_{e1} \div 12 g\right].$$

Line 8 is obtained by multiplication of line 5 by line 3 with the product multiplied by $12/\lambda$ to balance the factor $\lambda/12$ in line 7. For example, for station e, line 8 becomes

$$(1.000 \times 87.03 \times 12 \div 70.7)\left[(\omega_1^2 Z_{e1} \div g) \times \frac{\lambda}{12}\right].$$

Line 9 is obtained by addition of line 7 and line 8. At station e, line 9 is (45.55 + 14.77). The other lines follow the same procedures. Before leaving this discussion, note that the inertia load per unit length has a discontinuity in station 2. In this station, eqs. (3.1) and (3.3) are used.

IV. DYNAMIC STRUCTURAL PROPERTIES: SECOND AND HIGHER MODES

For the second and higher modes, the procedure outlined in Topic III is not a convergent process. This is because in processing any assumed mode shape, any impurity of the lower modes is magnified more than that of the higher mode. After a large number of repetitions it is found that the higher modes disappear altogether and that only the fundamental mode remains (6). However, the process can be modified a little by utilizing the suggestion made by Newmark that the modification requires purification of the lower harmonic impurities.

If the normal elastic curves of a system of length h are $Z_1(x), Z_2(x), \cdots Z_j(x)$, then any arbitrary deflection curve of that system can be developed into a series

$$Z(x) = \phi_1 Z_1(x) + \phi_2 Z_2(x) + \cdots + \phi_j Z_j(x) \qquad \cdots\cdots (4.1)$$

Moreover, the relation

$$\int_0^h m(x)\, Z_r(x)\, Z_s(x) = 0, \quad \text{if } r \neq s, \qquad \cdots\cdots (4.2)$$

holds, so that any coefficient ϕ_j in eq. (4.2) can be found to be

$$\phi_j = \frac{\int_0^h m(x)\, Z(x)\, Z_j(x)\, dx}{\int_0^h m(x)\, Z_j^2(x)\, dx}. \qquad \cdots\cdots (4.3)$$

Equations (4.1), (4.2), and (4.3) give a generalization of the theory of Fourier series. A rigorous proof of eq. (4.2) is found in (6). The proof is not necessary here because in the computations of the higher mode shapes, the orthogonality condition of eq. (4.2) has to be satisfied first.

Now, let $Z(x)$ be the assumed second mode which of course contains some first harmonic impurity, call it $A_1 Z_1(x)$. Then the purified second mode shape is

$$Z_2(x) = Z(x) - A_1 Z_1(x), \qquad \cdots\cdots (4.4)$$

which is free from first harmonic impurity. Substitute eq. (4.4) in eq. (4.2) and get

$$A_1 = \frac{\int_0^h m(x)\, Z(x)\, Z_1(x)\, dx}{\int_0^h m(x)\, Z_1^2(x)\, dx}. \qquad \cdots\cdots (4.5)$$

Again, Newmark's method of integration, with the regionally parabolic assumption of the curves $m(x)Z(x)Z_1(x)$ and $m(x)Z_1(x)$ is used in evaluating the numerator and denominator of eq. (4.5). The computations for A_1 are shown in Fig. 4.1. After finding the value of A_1, then the assumed deflection curve is purified. Each value of Z_1 is multiplied by A_1 as shown in Fig. 4.2 and then the corresponding $Z_1 A_1$ is subtracted from the assumed Z. The succeeding steps follow the same procedures discussed in Topic III.

The procedure is similar for the third mode. However, this time the assumed deflection curve has to be purified from both the first and second modes by the same orthogonality relationship of eq. (4.2). For the third mode, let the assumed deflection curve by Z(x), so that the purified deflection $Z_3(x)$ becomes

$$Z_3(x) = Z(x) - A_2 Z_1(x) - B_2 Z_2(x), \qquad \cdots\cdots (4.6)$$

where

Z(x) = assumed third mode deflection curve,
$Z_3(x)$ = purified assumed third mode deflection curve,
$Z_1(x)$ = from previous computations of first mode,
$Z_2(x)$ = from previous computations of second mode,

A_2 and B_2 are constants of purification. Substitution of eq. (4.6) into eq. (4.2) give

$$B_2 = \frac{\int_o^h m(x) Z(x) Z_2(x) dx}{\int_o^h m(x) Z_2^2(x) dx} , \qquad \ldots\ldots (4.7)$$

$$A_2 = \frac{\int_o^h m(x) Z(x) d(x) dx}{\int_o^h m(x) Z_1^2(x) dx} . \qquad \ldots\ldots (4.8)$$

The computations of the values of A_2 and B_2 by Newmark's method of integration are shown in Fig. 4.3. The computations of the derived third mode shape follow the same procedures for the first and second modes, only this time the assumed third mode shape is corrected for both the first and second harmonics by $-A_2Z_1(x)$ and by $-B_2Z_2(x)$ respectively, giving the purified assumed curve $Z_3(x)$ shown in Fig. 4.4. The natural frequency computations are the same for all modes. The procedure for higher modes is the same as the first three modes, i.e. the assumed higher mode is purified from the lower modes. The first three modes only are considered in this study.

Now, the constants Γ_j can be evaluated. The formula for Γ_j is given in eq. (2.23). The computations and results by using Newmark's method of integration are shown in Fig. 4.5.

Note that in the computations of the mode shapes, the shear V_j and bending moment factors M_j are automatically computed. The values of Z_j, V_j, and M_j for the 707' Clifty Creek (10) stack are plotted in Figs. 4.6, 4.7, and 4.8. The curves for the 605' modified Selby (11) and the 562' Kyger Creek (12) stacks are in (7).

V. GENERALIZED CO-ORDINATE RESPONSE TO EARTHQUAKE

The general equation for the generalized coordinate ϕ_j with the effect of ground-motion derived in Topic III is eq. (2.25). This equation can be solved either by the Laplace Transform method (13, 7), Newmark's step by step method (14, 7), or by the use of the analogue computer. Since the function $\ddot{y}_b$ does not follow a simple algebraic or trigonometric function, the analogue computer is used in this study.

The theory, design, and operation of the analogue computer can be found in the report of Howe, C. E., and Howe, R. E. (15). According to the above report, the basic computing element is the operational amplifier which can do three basic operations, namely: addition (summer), sign inversion (sign inverter), and integration (integrator). Besides the analogue computer, a function generator which is used to simulate the accelerograph is also used. The Reeves Electronic Analogue Computer (REAC Model No. C101), Reeves Function Generator (Model No. IC-101), and Brush Record are used in this study.

Since the range of the periods of chimneys is from 0.3 to 3.0 seconds, it is advisable to express eq. (2.25) in terms of a new variable t'. Let,

$$t' = \omega t . \qquad \ldots\ldots (5.1)$$

Then

$$\frac{d\phi}{dt} = \frac{d\phi}{dt'} \cdot \frac{dt'}{dt} = \omega \frac{d\phi}{dt'} , \qquad \ldots\ldots (5.2)$$

and

$$\frac{d^2\phi}{dt^2} = \frac{d}{dt}\left(\frac{d\phi}{dt}\right) = \frac{d}{dt}\left(\omega \frac{d\phi}{dt'}\right) = \frac{d}{dt'}\left(\omega \frac{d\phi}{dt'}\right)\frac{dt'}{dt} = \omega^2 \frac{d^2\phi}{dt'^2} \quad \ldots (5.3)$$

Similarly,

$$\frac{d^2 y_b}{dt^2} = \omega^2 \frac{d^2 y_b}{dt'^2} . \quad \ldots\ldots\ldots (5.4)$$

Therefore eq. (2.25) becomes

$$\frac{d^2\phi}{dt'^2} + 2\beta \frac{d\phi}{dt'} + \phi = -\frac{1}{\omega^2} \frac{d^2 y_b}{dt'^2} . \quad \ldots\ldots\ldots (5.5)$$

The computer circuit for eq. (5.5) is shown in Fig. 5.1. The response curves ϕ_j for the Clifty Creek Stack (h = 707'), whose first three periods are 3.0, 0.88, and 0.38 seconds per cycle, with damping coefficient β_j = 0.050 for each mode, and using the El Centro earthquake of May 18 with N-S component, are shown in Fig. 5.2.

VI. DESIGN SHEARS AND BENDING MOMENTS

From the results of Topics IV and V the instantaneous shears and bending moments can be computed by the use of eqs. (2.28) and (2.29). The procedure is as follows:

1. Multiply the first two dynamic structural properties to get $V_j \cdot \Gamma_j$ and $M_j \cdot \Gamma_j$ and express the results in terms of the maximum value which occurs at the base of the stack for the first mode. Call these quantities shear coefficients $(V_j \cdot \Gamma_j)$ and bending moment coefficients $(M_j \cdot \Gamma_j)$.
2. Multiply the results of step (1) by the response $\phi_j(t)$ at different instants as given in Topic V.
3. Plot the results of step (2) and obtain the maximum shears and bending moments at various points along the stack.

The Clifty Creek Stack is used as a numerical example, taking the base of the stack first. For the shear at the base,

$$V_{b1}\Gamma_1 = (593.6\lambda\omega_1^2 \div 12g)(2.048) = 1215.7\lambda\omega_1^2 \div 12g , \quad \ldots\ldots (6.1)$$

$$V_{b2}\Gamma_2 = (-452.5\lambda\omega_2^2 \div 12g)(-1.882) = 851.6\lambda\omega_2^2 \div 12g , \quad \ldots\ldots (6.2)$$

$$V_{b3}\Gamma_3 = (334.5\lambda\omega_3^2 \div 12g)(1.491) = 498.7\lambda\omega_3^2 \div 12g , \quad \ldots\ldots (6.3)$$

or

$$V_{b1}\Gamma_1 = 1.000\, V_{max}\,\omega_1^2 , \quad \ldots\ldots (6.1a)$$

$$V_{b2}\Gamma_2 = 0.701\, V_{max}\,\omega_2^2 , \quad \ldots\ldots (6.2a)$$

$$V_{b3}\Gamma_3 = 0.401\, V_{max}\,\omega_3^2 . \quad \ldots\ldots (6.3a)$$

Hence, the shear at the base at time t is

$$V_b(t) = 1.000 V_{max}\omega_1^2\phi_1(t) + 0.701 V_{max}\omega_2^2\phi_2(t) + 0.401 V_{max}\omega_3^2\phi_3(t) + \ldots . \quad \ldots (6.4)$$

The bending moment at the base is computed in the same manner,

$$M_{b1}\Gamma_1 = 1.000\, M_{max}\,\omega_1^2 , \quad \ldots\ldots (6.5)$$

$$M_{b2}\Gamma_2 = 0.316\, M_{max}\,\omega_2^2 , \quad \ldots\ldots (6.6)$$

$$M_{b3}\Gamma_3 = 0.111\, M_{max}\,\omega_3^2 . \quad \ldots\ldots (6.7)$$

Hence, the bending moment at the base of the 707-foot stack at time t is

$$M_b(t) = 1.000 M_{max}\omega_1^2\phi_1(t) + 0.316 M_{max}\omega_2^2\phi_2(t) + 0.111 M_{max}\omega_3^2\phi_3(t) + \ldots . \quad \ldots (6.8)$$

The shear coefficients $(V_i \Gamma_i)$ and the bending moment coefficients $(M_i \Gamma_i)$ are tabulated in Tables 6.1 and 6.2. The instantaneous shears and bending moments at different heights along the illustrative stack (Clifty Creek) discussed previously are plotted in Figs. 6.1 and 6.2.

VII. CONCLUSIONS AND DESIGN RECOMMENDATIONS

The shears and bending moments along the height of the chimneys are computed by the use of the empirical seismic coefficient K_e for a particular locality. The seismic coefficient is multiplied by the weight of the chimney above the section under consideration to get the forces.

The maximum shears and bending moments along the height of the stack obtained in Topic VI are also plotted. Then these maximum shears and bending moments are divided by the shears and bending moments derived by the use of the seismic coefficient. The result of the division is defined as the magnification factor. The results of the computations are shown in Figs. 7.1 and 7.2. Figs. 7.3 and 7.4 show that the shear and bending moment magnification factor curves for damping coefficient of $7\frac{1}{2}\%$ are below the curves for 5% but the deviation is not significant enough to affect the recommended design formulas. The magnification factors corresponding to $(1+\frac{h}{100})$ based on the ACI Code (16) Title No. 49-26 are plotted. These magnification factors are compared with the ones obtained by means of the dynamic analyses made in this study. The ACI Code is found to be insufficient as shown in Fig. 7.5, for regions where strong-motion earthquakes occur even if the value of $K_e = 0.20$ is used. Therefore, new formulas for the magnification factors need to be derived.

An envelope is drawn for the magnification factor curves, and parabolic fitted curves are obtained and recommended for preliminary design. The fitted curves are shown in Figs. 7.3 and 7.5. Other fitted curves are in (7).

After the formulas for the magnification factors have been derived, it is necessary to assign values to the seismic coefficients K_e for different localities. The ideal thing to do is to make similar studies of available accelerograph records of earthquakes for the particular locality and then determine K_e. However, in the absence of accelerograph records, the engineer is referred to the map showing occurrences of earthquakes of various intensities for different localities in the U. S. put out by the American Standards Association (17). In this study, earthquake regions are divided into three groups, namely:

1. Strong-motion region ($K_e = 0.20$), where the accelerograph records show maximum accelerations of from 0.09g to 0.33g,
2. Medium-intensity region ($K_e = 0.06$), where the accelerograph records show maximum accelerations of from 0.05g to 0.09g,
3. Light-intensity region ($K_e = 0.03$), where the accelerograph records show maximum accelerations of less than 0.05g.

The recommended design formulas for the shears and bending moments (see the end of paper for nomenclature) are:

$$V = W' K_e h'' \left[1.8 + 8\left(\frac{x - .5h}{.5h}\right)^2\right], \quad x \geq .5h, \qquad \ldots . (7.1)$$

$$= 1.8 W' K_e h'', \quad x \leq .5h, \qquad \ldots . (7.2)$$

$$M = W' K_e h'' \left[1 + 8\left(\frac{x - .2h}{.8h}\right)^2\right], \quad x \geq .2h, \qquad \ldots . (7.3)$$

$$= W' K_e h'', \quad x \leq .2h, \qquad \ldots . (7.4)$$

for stacks whose fundamental periods are from 2.4 to 3.0 seconds per cycle.

The author would like to thank Professor B. G. Johnston and Professor L. C. Maugh for their close supervision, and through whose research projects the author gained the experience which provided the necessary background for this study; Professor G. E. Hay, for his assistance in the mathematical analysis; Professor G. E. Hansen for his help in the mechanics of vibration; Professor R. H. Sherlock and Professor L. M. Legatski for valuable suggestions; the Department of Aeronautical Engineering, University of Michigan, for the use of its analogue computer; Smith, Hinchman, and Grylls, Inc., of Detroit, Michigan, and my wife Beatriz for their help in the preparation of the manuscript.

BIBLIOGRAPHY

1. Alford, J. L., Housner, G. W., and Martel, R. R. "Spectrum Analyses of Strong-Motion Earthquakes," First Technical Report under Office of Naval Research, Contract N6onr-244, California Institute of Technology, Pasadena, California, August, 1951.

2. Hisada, T. "Nonlinear Vibrations of Two Story Buildings," Transactions of the Architectural Institute of Japan, March, 1955.

3. Merritt, R. G. "Effect of Foundation Compliance on the Earthquake Stresses in Typical Tall Buildings", Thesis, California Institute of Technology, Pasadena, California, 1952.

4. White, M. P. "Friction in Buildings: Its Magnitude and Its Importance in Limiting Earthquake Stresses", Bull. Seism. Soc. Amer., Vol. 31, pp. 93-99, 1941.

5. Timoshenko, S. P. "Vibration Problems in Engineering", D. Van Nostrand Co., Inc., New York, 2nd ed., 1937.

6. Den Hartog, J. P. "Mechanical Vibrations", McGraw-Hill Book Co., Inc., New York, 3rd ed., 1947.

7. Isada, N. M. "Design and Analyses of Tall Tapered Reinforced Concrete Chimneys Subjected to Earthquake", Thesis, University of Michigan, Ann Arbor, 1955.

8. Bleich, F. "Buckling Strength of Metal Structures", McGraw-Hill Book Co., Inc., New York, 1952.

9. Johnston, B. G., "C.E. 231 Lecture Notes", University of Michigan,

Spring, 1952.

10. Maugh, L. C. and Legatski, L. M. "Structural Behavior of the Reinforced Concrete Stacks of the Clifty Creek Power Plant", Engineering Research Institute, University of Michigan, Ann Arbor, Project 2151, 1953.

11. Amer. Smelting and Refining Co. "Chimney Height Sets Record", Engineering News Record, Vol. 119, p. 1040, 1937.

12. Maugh, L. C., and Legatski, L. M. "Structural Behavior of the Reinforced Concrete Stacks of the Kyger Creek Power Plant", Engineering Research Institute, University of Michigan, Ann Arbor, Project 2182, 1953.

13. Churchill, R. V. "Modern Operational Mathematics in Engineering", McGraw-Hill Book Co., Inc., New York, 1944.

14. Newmark, N. M. "Methods of Analysis for Structures Subjected to Dynamic Loading", Directorate of Intelligence, U.S. Air Force, Washington, D. C., 1950.

15. Howe, C. E. and Howe, R. M. "A Tabletop Electronic Differential Analyzer", Department of Aeronautical Engineering, University of Michigan, Ann Arbor, October, 1953.

16. Amer. Concrete Institute Committee 505 "Proposed Standard Specification for the Design and Construction of Reinforced Concrete Chimneys", Journal of the Amer. Concrete Institute, Vol. 24, pp. 353-400, January, 1953.

17. Amer. Standards Association, "Minimum Design Loads in Buildings and Other Structures", Amer. Standards Association, New York, 1945.

18. Maugh, L. C., Rumman, W., Isada, N. M. "Structural Behavior of the 325-foot Steel Stack for Unit No. 6, Glen Lyn Plant", Engineering Research Institute, University of Michigan, Ann Arbor, Project 2371, 1955.

19. Johnston, B. G., Isada, N. M. "A Design and Analysis of a Building Subjected to Atomic Blast", Engineering Research Institute, University of Michigan, Ann Arbor, Project 1106, 1956.

NOMENCLATURE

Units Used

Kip-foot units where 1 kip = 1,000 lbs.

Latin Letter Symbols

A_1, A_2, B_2 mode shape purifying constants

a, b, c	ordinates of parabolic curve
E	Young's modulus of elasticity
g	acceleration due to gravity
h	height of stack
h'	distance from section under consideration to the section that is 1/5 of the total height of the chimney above base
h''	distance from section under consideration to center of gravity of chimney mass above the section
h''_v'	shear magnification factors
h''_m'	bending moment magnification factors
I	moment of inertia
K_e	seismic coefficient
M_j	bending moment factor
$M_j \Gamma_j$	bending moment coefficient
M	bending moment
m	mass per unit length
Q_j	generalized force corresponding to q_j
q_j	generalized co-ordinates which are functions of time alone
R	vertical reactions
T	total kinetic energy of entire vibrating system
t	time variable
$t' = \omega t$	new time variable
U	total potential energy of entire vibrating system
V_j	shear factor
$V_j \Gamma_j$	shear coefficient
V	shear
W	load per unit length along the beam or stack

W' weight of chimney above section under consideration, including any portion of lining supported from the chimney shell

w weight per unit length along the beam or stack

x distance from base to a general point P on neutral axis

Y absolute horizontal deflection of mass

y relative horizontal deflection of the mass with respect to the ground

y_b horizontal motion of the base of the beam or stack

Z_j mode shape or characteristic function

Greek Letter Symbols

β_j ratio of assigned damping to critical damping

Δ denotes increment

Γ_j dynamic structural constant

θ slope of the beam

λ length of a segment of a stack

τ_j natural period in seconds per cycle

ω_j natural frequency in radians per second

Subscripts and Superscripts

j refers to the mode of vibration

b refers to the base of the stack

e refers to the top of the stack

r subscript for the rth mode of vibration

s subscript for the sth mode of vibration

$\dot{q}$ $\partial q/\partial t$

$\dot{y}$ $\partial y/\partial t$

$\dot{Z}$ $\partial Z/\partial x$

$\ddot{Z}$ $\partial^2 Z/\partial x^2$

ϕ_j q_i/Γ_j

Table 6.1

Shear Coefficients

Stack → x ÷ h	Clifty Creek h = 707' V_1 $\lceil_1$	V_2 $\lceil_2$	V_3 $\lceil_3$	Modified Selby h = 605' V_1 $\lceil_1$	V_2 $\lceil_2$	V_3 $\lceil_3$	Kyger Creek h = 562' V_1 $\lceil_1$	V_2 $\lceil_2$	V_3 $\lceil_3$
1.00									
.95	.102	-.080	.055	.089	-.075	.048	.093	-.079	.057
.85	.298	-.179	.063	.267	-.173	.070	.306	-.190	.084
.75	.451	-.171	-.019	.431	-.177	-.007	.487	-.181	-.011
.65	.596	-.081	-.115	.580	-.091	-.113	.624	-.084	-.120
.55	.728	.076	-.150	.706	.060	-.156	.731	.070	-.169
.45	.826	.250	-.091	.805	.240	-.105	.816	.255	-.125
.35	.900	.416	.043	.885	.427	.031	.888	.461	.015
.25	.956	.568	.216	.950	.604	.217	.950	.674	.239
.15	.989	.665	.351	.984	.711	.352	.989	.825	.439
.05	1.000	.701	.410	1.000	.762	.425	1.000	.872	.512
0									
	Factor = $7162\omega_j^2$ + g kips/ft			Factor = $3849\omega_j^2$ + g kips/ft			Factor = $4413\omega_j^2$ + g kips/ft		

Table 6.2

Bending Moment Coefficients

Stack →	Clifty Creek h = 707'			Modified Selby h = 605'			Kyger Creek h = 562'		
x + h	$M_1\Gamma_1$	$M_2\Gamma_2$	$M_3\Gamma_3$	$M_1\Gamma_1$	$M_2\Gamma_2$	$M_3\Gamma_3$	$M_1\Gamma_1$	$M_2\Gamma_2$	$M_3\Gamma_3$
1.0	0	0	0	0	0	0	0	0	0
.9	.015	-.012	.008	.013	-.011	.007	.014	-.011	.008
.8	.058	-.038	.017	.053	-.037	.018	.058	-.039	.021
.7	.124	-.063	.014	.118	-.064	.016	.129	-.065	.019
.6	.211	-.075	-.002	.204	-.077	-.001	.219	-.078	.002
.5	.318	-.064	-.024	.310	-.068	-.024	.326	-.067	-.023
.4	.438	-.027	-.037	.430	-.032	-.040	.444	-.030	-.041
.3	.570	.033	-.031	.562	.032	-.035	.573	.036	-.039
.2	.709	.116	0	.704	.122	-.002	.711	.134	-.004
.1	.854	.214	.051	.851	.228	.050	.855	.253	.060
0	1.000	.316	.111	1.000	.342	.114	1.000	.380	.134
	Factor = $3{,}467{,}000\,\omega_j^2$ + ft-kips/ft			Factor = $1{,}560{,}000\,\omega_j^2$ + g ft-kips/ft			Factor = $1{,}708{,}000\,\omega_j^2$ + g ft-kips/ft		

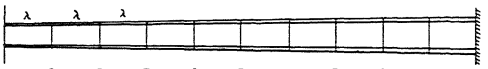

	e	9	8	7	6	5	4	3	2	1	b	MULTIPLIER Ft.–kip units
1) Station												
2) Weight (w)	7.5	9.5	11.4	15.1	20.3	23.1	29.1	42.1	70.0 42.1	52.0	76.5	Kips per ft.
3) " Conc.	87.03	191.08	72.03	71.90	77.34	86.69	95.30	149.00	427.48	2355.87		Added Wt. (Kips)
4) EI	1.00	1.55	2.70	5.20	9.25	12.95	20.70	35.80	51.85	69.25	115.90	EI_g
5) Assumed Z_1	1.000	.799	.610	.445	.309	.199	.119	.063	.026	.006	0	Z_{g1}
6) Inertia Load Int.	7.500	7.591	6.954	6.720	6.273	4.597	3.463	2.652	1.820 1.095	0.312	0	$\omega_1^2 Z_{g1} \div g$
7) Conc. In. Load	45.55	90.36	83.85	80.43	74.05	55.71	41.88	31.80	17.36	4.22		$\lambda\omega_1^2 Z_{g1} \div 12g$
8) " " "	14.77	25.91	7.46	5.43	4.06	2.93	1.92	1.59	1.89	2.40		Do
9) Avg. Shear (V)		60.32	176.59	267.90	353.76	431.87	490.51	534.31	567.70	586.95	593.57	Do
10) Moment (M)	0	60.3	236.9	504.8	858.6	1290.4	1781.0	2315.3	2883.0	3470.0	4063.5	$\lambda^2\omega_1^2 Z_{g1} \div 12g$
11) M ÷ EI (ϕ)	0	38.90	87.74	97.08	92.82	99.64	86.04	64.67	55.60	50.11	35.06	$\lambda^2\omega_1^2 Z_{g1} \div 12EI_g g$
12) Conc. ϕ		476.7	1013.4	1151.4	1124.9	1175.3	1024.7	788.3	670.8	591.8	245.2	$\lambda^3\omega_1^2 Z_{g1} \div 144EI_g g$
13) Avg. Slope Σ		8263	7786	6772	5621	4496	3321	2296	1508	837	245	Do
14) Deflection $\Sigma\Sigma$	41145	32882	25096	18324	12703	8207	4886	2590	1082	245	0	$\lambda^4\omega_1^2 Z_{g1} \div 144EI_g g$
15) Relative Z_1	1.000	.799	.610	.445	.309	.199	.119	.063	.026	.006	0	Z_{g1}
16) Relative V_1		.102	.298	.451	.596	.728	.826	.900	.956	.989	1.000	V_{b1}
17) Relative M_1	0		.015	.058	.124	.211	.318	.438	.570	.709	.854	1.00 M_{b1}
18) ω_1^2	4.54	4.54	4.54	4.54	4.54	4.54	4.54	4.54	4.54	4.54	4.54	(radians per sec.)^2

Deflection Multiplier = $(\lambda^4\omega_1^2 Z_{g1}) \div (144EI_g g) = (70.4^4\omega_1^2 Z_{g1}) \div (144 \cdot 3.5 \cdot 144 \cdot 1000 \cdot 2000 \cdot 32.2) = 5.35 \cdot 10^{-6}\omega_1^2 Z_{g1}$

Average First Mode Frequency ω_1 = 2.13 radians per second

" " " Period τ_1 = 2.95 seconds per cycle

FIG. 3.1. CALCULATIONS OF FIRST MODE DYNAMIC PROPERTIES.

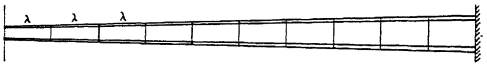

Station	e	9	8	7	6	5	4	3	2	1	b	MULTIPLIER Ft.–kip units
Weight (w)	7.5	9.5	11.4	15.1	20.3	23.1	29.1	42.1	70.0 42.1	52.0	76.5	Kips per ft.
" Conc.	87.03	191.08	72.03	71.90	77.34	86.69	95.30	149.00	427.48	2355.87		Added Wt. (kips)
Z_1	1.000	.799	.610	.445	.309	.199	.119	.063	.026	.006	0	Z_{g1}
Z_1^2	1.000	.638	.372	.198	.095	.040	.014	.004	.001	0	0	Z_{g1}^2
mZ_1^2	7.500	6.061	4.241	2.990	1.929	.924	.407	.168	.070 .042	0	0	$Z_{g1}^2 \div g$
Conc. mZ_1^2	42.31	72.55	51.46	36.07	23.20	11.58	5.16	2.16	0.81	0.04		$\lambda Z_{g1}^2 \div 12g$
" "	14.77	20.69	4.55	2.42	1.25	0.59	0.23	0.10	0.07	0	0	Do
Σ(Conc. mZ_1^2)	57.08	150.12	206.13	244.62	269.07	281.24	286.63	288.89	289.77	289.81		Do
	$\int_0^h mZ_1^2 dx$ = 289.81(Do)											
Assumed Z_2	1.000	.433	−.026	−.297	−.397	−.381	−.293	−.183	−.086	−.021	0	Z_{g2}
Z_1Z_2	1.000	.346	−.016	−.132	−.123	−.076	−.035	−.012	−.002	−.00013	0	$Z_{g1}Z_{g2}$
mZ_1Z_2	7.500	3.287	−.182	−1.993	−2.497	−1.756	−1.019	−.505	−.140 −.084	−.007	0	$Z_{g1}Z_{g2} \div g$
Conc. mZ_1Z_2	36.202	40.188	−0.526	−22.609	−28.719	−21.076	12.451	−6.209	−1.810	−0.154		$\lambda Z_{g1}Z_g \div 12g$
" "	14.772	11.222	−0.196	−1.611	−1.615	−1.118	−0.566	−0.303	−0.145	−0.050		Do
Σ(Conc. mZ_1Z_2)	50.974	102.384	101.662	77.442	47.108	24.914	11.897	5.385	3.430	3.226		Do
	$\int_0^h mZ_1Z_2 dx$ = 3.226(Do)											

Since $Z_{g1} = Z_{g2}$ = unity, then $A_1 = \dfrac{\int_0^h mZ_1Z_2\,dx}{\int_0^h mZ_1^2\,dx} = \dfrac{3.226}{289.81} = +0.01113$

FIG. 4.1. SECOND MODE ORTHOGONALITY CALCULATIONS.

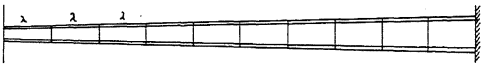

Station	e	9	8	7	6	5	4	3	2	1	b	MULTIPLIER Ft.–kip units
Weight (w)	7.5	9.5	11.4	15.1	20.3	23.1	29.1	42.1	70.0 42.1	52.0	76.5	kips per ft.
" Conc.	87.03	191.08	72.03	71.90	77.34	86.69	95.30	149.00	427.48	2355.87		Added Wt. (kips)
EI	1.00	1.55	2.70	5.20	9.25	12.95	20.70	35.80	51.85	69.25	115.90	EI_g
Assumed Z_2	1.000	.433	−.026	−.297	−.397	−.381	−.293	−.183	−.086	−.021	0	Z_{g2}
A_1Z_1	.011	.009	.007	.005	.003	.002	.001	.001	0	0	0	Z_{g1}
Purified Z_2	.989	.424	−.033	−.302	−.401	−.383	−.294	−.184	−.086	−.021	0	Z_{g2}
Relative Purified Z_2	1.000	.429	−.033	−.305	−.405	−.387	−.297	−.186	−.087	−.021	0	Z_{g2}
Inertia Ld. Int.	7.500	4.076	−.376	−4.606	−8.222	−8.940	−8.643	−7.831	−6.090 −3.663	−1.092	0	$\omega_2^2 Z_{g2} \div g$
Conc. In. Load	38.666	47.884	−4.290	−54.658	−95.766	−106.265	−103.201	−93.043	−56.583	−14.583		$\lambda\omega_2^2 Z_{g2} \div 12g$
" " "	14.772	13.913	−.403	−3.722	−5.316	−5.694	−4.804	−4.704	−6.312	−8.397	0	Do
Avg. Shear (V)		53.438	115.235	110.542	52.162	−48.920	−160.879	−268.884	−366.631	−429.526	−452.506	Do
Moment (M)	0	53.438	168.673	279.215	331.377	282.457	121.578	−147.306	−513.937	−943.446	−1395.97	$\lambda^2\omega_2^2 Z_{g2} \div 12g$
M ÷ EI (ϕ)	0	34.476	62.471	53.695	35.825	21.811	5.873	−4.115	−9.912	−13.624	−12.045	$\lambda^2\omega_2^2 Z_{g2} \div 12EI_g g$
Conc. ϕ		407.231	712.881	635.246	433.756	259.808	76.426	−45.389	−116.859	−158.197	−78.074	$\lambda^3\omega_2^2 Z_{g2} \div 144EI_g g$
Avg. Slope Σ		2127.029	1719.798	1006.917	371.671	−62.085	−321.893	−398.319	−353.130	−236.271	−78.074	Do
Deflection $\Sigma\Sigma$	3775.64	1648.61	−71.18	−1078.10	−1449.77	−1387.69	−1065.79	−667.48	−314.35	−78.07	0	$\lambda^4\omega_2^2 Z_{g2} \div 144EI_g g$
Relative Z_2	1.000	.437	−.019	−.286	−.384	−.368	−.282	−.177	−.083	−.021	0	Z_{g2}
Relative V_2		.118	.255	.244	.115	−.108	−.356	−.594	−.810	−.949	−1.000	V_{b2}
Relative M_2	0		.038	.121	.200	.237	.202	.087	−.106	−.368	−.676	−1.00 M_{b2}
ω_2^2	49.6	49.6	49.6	49.6	49.6	49.6	49.6	49.5	49.6	49.5	49.6	(radians per second)^2

Deflection Multiplier = $5.35 \cdot 10^{-6}\omega_2^2 Z_{g2}$, from Fig. 3.2.

Average Second Mode Frequency ω_2 = 7.05 radians per second

" " " Period τ_2 = 0.88 second per cycle

FIG. 4.2. CALCULATIONS OF SECOND MODE DYNAMIC PROPERTIES.

Third Mode

Station	e	9	8	7	6	5	4	3	2	1	b	MULTIPLIER Ft.-kip units
Weight (w)	7.5	9.5	11.4	15.1	20.3	23.1	29.1	42.1	70.0 / 42.1	52.0	76.5	Kips per ft.
" Conc.	87.03	191.08	72.03	71.90	77.34	86.69	95.30	149.00	427.48	235	5.87	Added Wt. (kips)
Z_z	1.000	.429	−.033	−.305	−.405	−.387	−.297	−.186	.087	−.021	0	Z_{e3}
Z_z^2	1.000	.184	.001	.093	.164	.150	.088	.035	.008	.00044	0	Z_{e2}^2
mZ_z^2	7.500	1.748	.011	1.404	3.329	3.465	2.561	1.474	.560 / .337	.023	0	$Z_{e3}^2 \div g$
Conc. mZ_z^2	31.49	24.99	3.26	17.38	38.16	40.54	30.55	17.86	6.35	0.57		$\lambda Z_{e3}^2 \div 12g$
" "	14.77	5.97	0.01	1.14	2.15	2.21	1.42	0.89	0.58	0.18	0	Do
$\sum$(Conc. mZ_z^2)										240.47		Do

$$\int_o^h mZ_z^2\,dx = 240.47(Do)$$

Assumed Z_y	1.000	−.053	−.604	−.536	−.178	.162	.319	.292	.171	.049	0	Z_{e3}
$Z_y Z_z$	1.000	−.023	.020	.163	.072	−.063	−.095	−.054	−.015	−.001	0	$Z_{e2} Z_{e3}$
$mZ_y Z_z$	7.500	−.219	.228	2.461	1.462	−1.455	−2.765	−2.273	−1.050 / −.632	−.052	0	$Z_{e2} Z_{e3} \div g$
Conc. $mZ_y Z_z$	25.48	5.54	4.52	26.30	15.63	−15.85	−31.38	−26.55	−11.48	−1.15	0	$\lambda Z_{e2} Z_{e3} \div 12g$
" "	14.77	−.75	.24	1.99	.95	−.93	−1.54	−1.37	−1.09	−.40		Do
$\sum$(Conc. $mZ_y Z_z$)										2.93		Do

Since $Z_{e2} = Z_{e3}$ = unity, then $B_z = (2.93) \div (240.47) = +0.012184$

Z_1	1.000	.799	.610	.445	.309	.199	.119	.063	.026	.006	0	Z_{e1}
$Z_1 Z_3$	1.000	−.042	−.368	−.239	−.055	.032	.038	.018	.004	.0003	0	$Z_{e1} Z_{e3}$
$mZ_1 Z_3$	7.500	−.399	−4.195	−3.609	−1.117	.739	1.406	.758	.280 / .168	.016	0	$Z_{e1} Z_{e3} \div g$
Conc. $mZ_1 Z_3$	27.15	−.69	−45.96	−41.40	−14.04	7.38	12.56	8.97	3.34	.33		$Z_{e1} Z_{e3} \div 12g$
" "	14.77	−1.36	−4.50	−2.92	−.72	.47	.61	.45	.29	.12	0	Do
$\sum$(Conc. $mZ_1 Z_3$)										−35.15		Do

Since $Z_{e1} = Z_{e3}$ = unity, then $A_z = (-35.15) \div (289.81) = -0.12129$

FIG. 4.3. THIRD MODE ORTHOGONALITY CALCULATIONS.

Third Mode

Station	e	9	8	7	6	5	4	3	2	1	b	MULTIPLIER Ft.-kip units
Weight (w)	7.5	9.5	11.4	15.1	20.3	23.1	29.1	42.1	70.0 / 42.1	52.0	76.5	kips per ft.
" Conc.	87.03	191.08	72.03	71.90	77.34	86.69	95.30	149.00	427.48	235	5.87	Added Wt. (kips)
EI	1.00	1.55	2.70	5.20	9.25	12.95	20.70	35.80	51.85	69.25	115.90	EI_e
Assumed Z_y	1.000	−.053	−.604	−.536	−.178	.162	.319	.292	.171	.049	0	Z_{e3}
$A_z Z_1$	−.121	−.097	−.074	−.054	−.037	−.024	−.014	−.008	−.003	−.001	0	Z_{e1}
$B_z Z_2$	.012	.005	0	−.004	−.005	−.005	−.004	−.002	−.001	0	0	Z_{e2}
Purified Z_y	1.109	.039	−.530	−.478	−.136	.191	.337	.302	.175	.050	0	Z_{e3}
Relative Purified Z_y	1.000	.035	−.478	−.431	−.123	.172	.304	.272	.158	.045	0	Z_{e3}
Inertia Load Int.	7.500	.333	−5.449	−6.508	−2.497	3.973	8.846	11.451	11.060 / 6.632	2.340	0	$\omega_3^2 Z_{e3} \div g$
Conc. Inertia Load	29.974	5.381	−60.665	−73.026	−27.505	46.079	103.884	134.416	98.942	30.052		$\lambda \omega_3^2 Z_{e3} \div 12g$
" " "	14.772	1.135	−5.844	−5.260	−1.615	2.531	4.917	6.883	11.464	17.994		Do
Avg. Shear (V)		44.746	51.562	−15.247	−93.533	−122.653	−74.043	34.758	176.057	286.463	334.509	Do
Moment (M)	0	44.746	96.008	80.761	−12.772	−135.425	−209.468	−174.710	1.347	287.810	622.319	$\lambda^2 \omega_3^2 Z_{e3} \div 12g$
$M \div EI$ (ϕ)	0	28.868	35.559	15.531	−1.381	−10.458	−10.119	−4.880	.026	4.156	5.369	$\lambda^2 \omega_3^2 Z_{e3} \div 12 EI_{eg}$
Concentrate ϕ		324.239	399.989	189.488	−8.737	−116.080	−116.528	−58.983	−.464	46.955	31.247	$\lambda^3 \omega_3^2 Z_{e3} \div 144 EI_{eg}$
Avg. Slope $\sum$		691.126	366.887	−33.102	−222.590	−213.853	−97.773	18.755	77.738	78.202	31.247	Do
Deflection $\sum$	696.637	5.511	−361.376	−328.274	−105.684	108.169	205.942	187.187	109.449	31.247	0	$\lambda^2 \omega_3^2 Z_{e3} \div 144 EI_{eg}$
Relative Z_y	1.000	.008	−.519	−.471	−.152	.155	.296	.269	.157	.045	0	Z_{e3}
Relative V_y	.134	.153	−.046	−.280	−.367	−.221	.104	.526	.856	1.000		V_{bz}
Relative M_y	0	.072	.154	.130	−.021	−.218	−.337	−.281	.002	.462	1.00	M_{bz}
ω_3^2	269	269	269	269	269	268	269	269	268	269		(radians per second)^2

Average Third Mode Frequency ω_3 = 16.4 radians per second

" " " Period τ_3 = 0.38 second per cycle

FIG. 4.4. CALCULATIONS OF THIRD MODE DYNAMIC PROPERTIES.

Station	e	9	8	7	6	5	4	3	2	1	b	MULTIPLIER Ft.-kip units
Weight (w)	7.5	9.5	11.4	15.1	20.3	23.1	29.1	42.1	70.0 / 42.1	52.0	76.5	Kips per ft.
" Conc.	87.03	191.08	72.03	71.90	77.34	86.69	95.30	149.00	427.48	235	5.87	Added Wt. (kips)
Z_y	1.000	.035	−.478	−.431	−.123	.172	.304	.272	.158	.045	0	Z_{e3}
Z_y^2	1.000	.001	.228	.186	.015	.030	.092	.074	.025	.002	0	Z_{e3}^2
mZ_y^2	7.500	.010	2.599	2.809	.305	.693	2.677	3.115	.750 / .053	.104	0	$Z_{e3}^2 \div g$
Conc. mZ_y^2	24.98	10.20	28.81	30.99	6.55	9.91	30.58	35.58	18.13	2.09		$\lambda Z_{e3}^2 \div 12g$
" "	14.77	.03	2.79	2.27	.20	.44	1.49	1.87	1.81	.80		Do
$\sum$(Conc. mZ_y^2)										224.29		Do

$$mZ\ dx = 224.29(Do)$$

From FIG. 4.4, $\int_o^h mZ_y\,dx = 334.51(Do)$, from FIG. 4.5, $\int_o^h mZ_y^2\,dx = 224.29(Do)$,

from FIG. 4.2, $\int_o^h mZ_z\,dx = -452.51(Do)$, from FIG. 4.3, $\int_o^h mZ_z^2\,dx = 240.47(Do)$,

from FIG. 3.2, $\int_o^h mZ_1\,dx = 593.57(Do)$, from FIG. 4.1, $\int_o^h mZ_1^2\,dx = 289.81(Do)$,

and $Z_{e3} = Z_{e2} = Z_{e1}$ = unity, therefore

$$\Gamma_1 = \int_o^h mZ_1\,dx \div \int_o^h mZ_1^2\,dx = 593.57 \div 289.81 = +2.048$$

$$\Gamma_2 = \int_o^h mZ_2\,dx \div \int_o^h mZ_2^2\,dx = -452.51 \div 240.47 = -1.882$$

$$\Gamma_3 = \int_o^h mZ_3\,dx \div \int_o^h mZ_3^2\,dx = 334.51 \div 224.29 = +1.491$$

FIG. 4.5. CALCULATIONS OF THE Γ_j QUANTITIES.

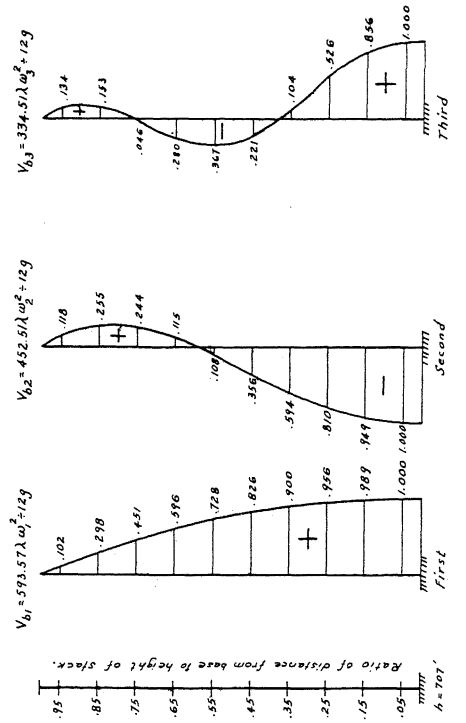

FIG. 4.7. SHEAR FACTORS.
CLIFTY CREEK STACK.

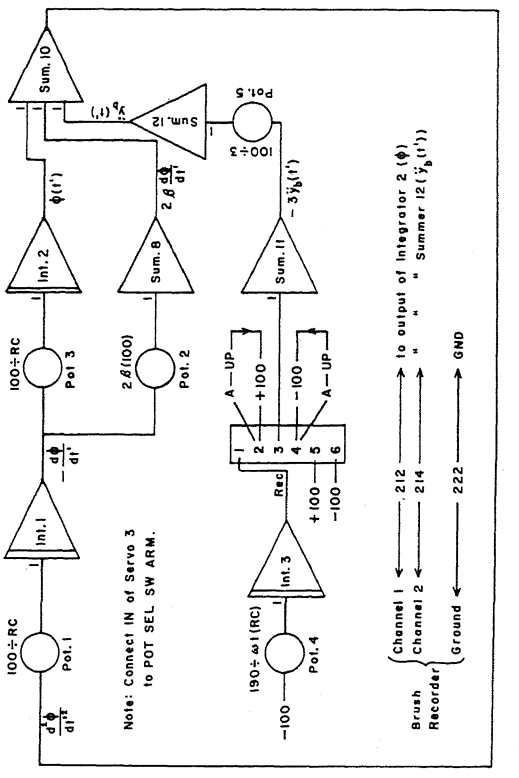

FIG. 5.1. ANALOG COMPUTER CIRCUIT.

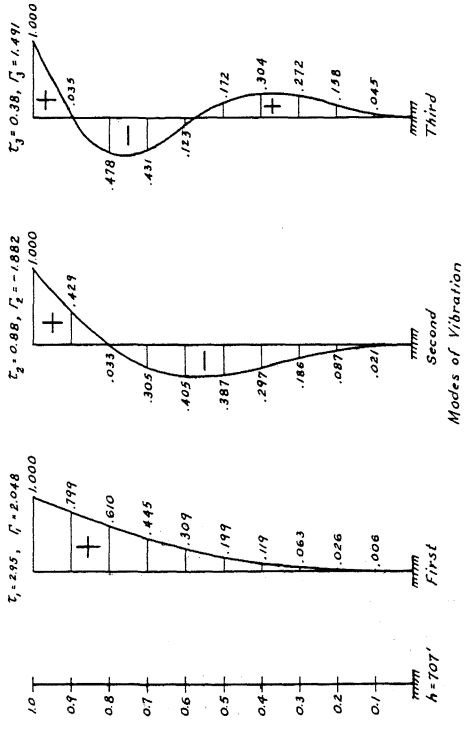

FIG. 4.6. DEFLECTION FACTORS.
CLIFTY CREEK STACK.

FIG. 4.8. BENDING MOMENT FACTORS.
CLIFTY CREEK STACK.

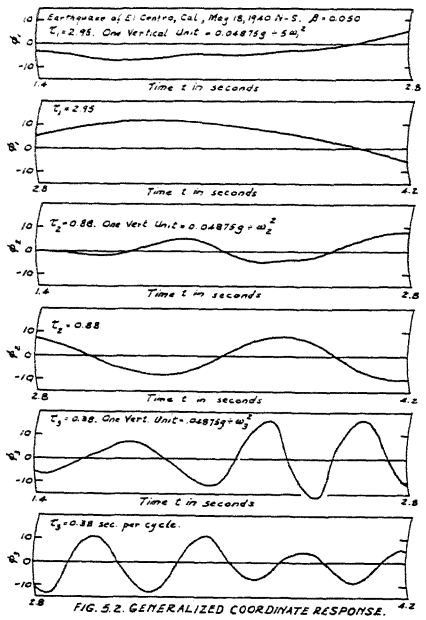

FIG. 5.2. GENERALIZED COORDINATE RESPONSE.

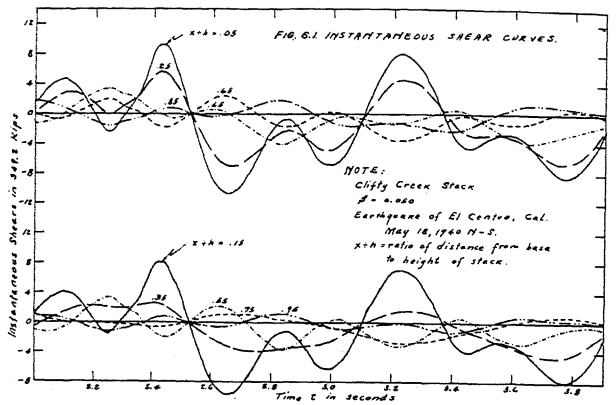

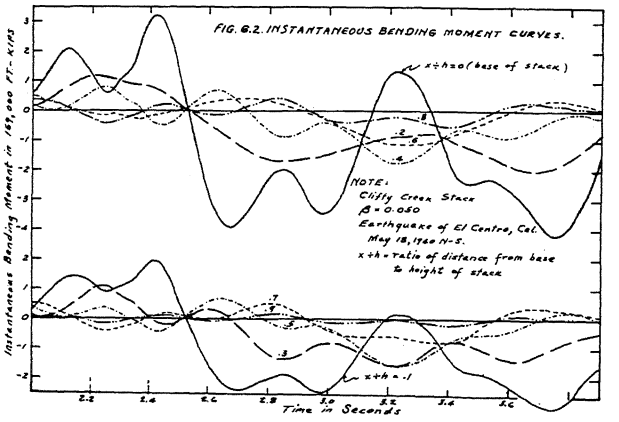

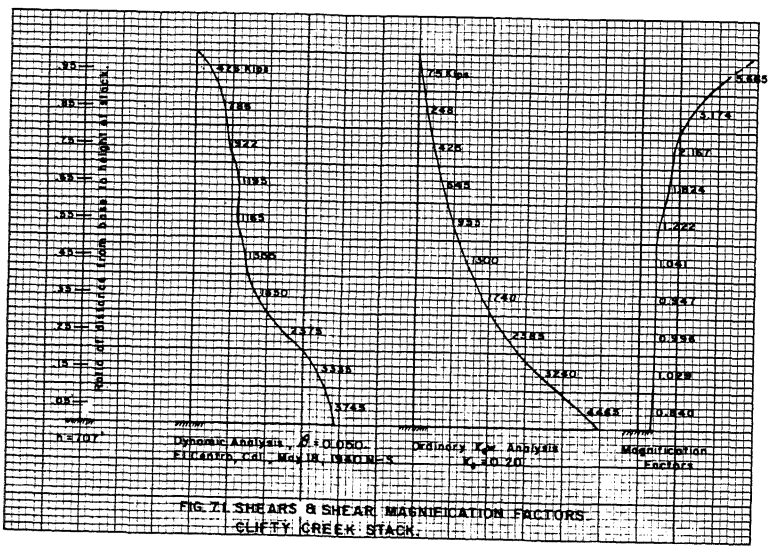

FIG. 7.1. SHEARS & SHEAR MAGNIFICATION FACTORS. CLIFTY CREEK STACK.

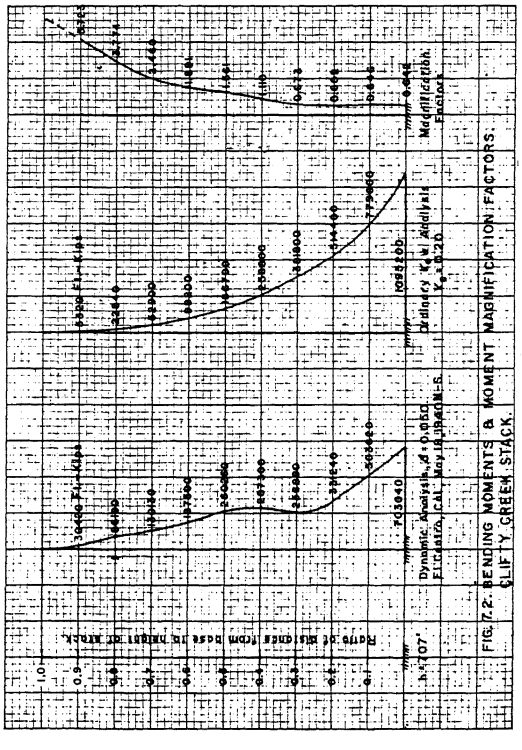

FIG. 7.2: BENDING MOMENTS & MOMENT MAGNIFICATION FACTORS CLIFTY GREEN STACK.

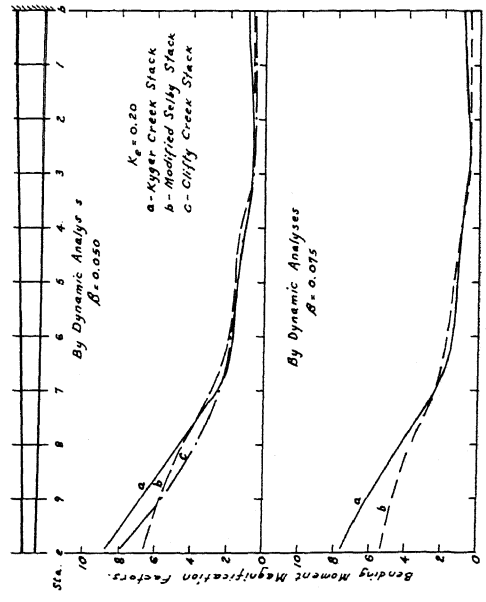

FIG. 7.4 BENDING MOMENT MAGNIFICATION FACTORS FOR REGIONS OF STRONG-MOTION EARTHQUAKES FOR 5% & 7.5 % OF CRITICAL DAMPING.

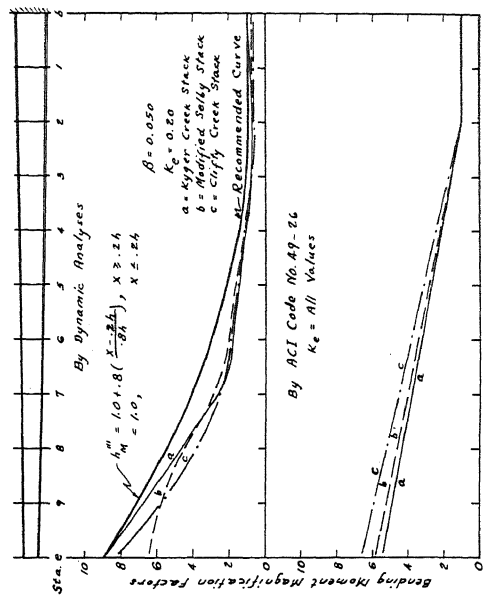

FIG. 7.5. BENDING MOMENT MAGNIFICATION FACTORS FOR REGIONS OF STRONG-MOTION EARTHQUAKES COMPARED TO ACI CODE NO. 49-26.

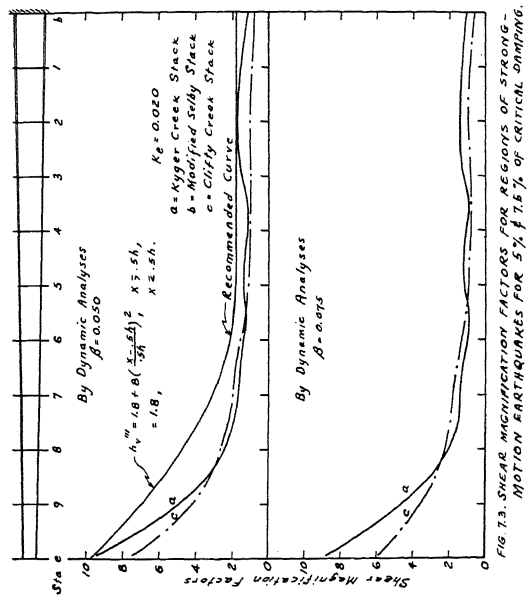

FIG. 7.3. SHEAR MAGNIFICATION FACTORS FOR REGIONS OF STRONG-MOTION EARTHQUAKES FOR 5% & 7.5 % OF CRITICAL DAMPING.